ASSESSMENT OF A COOLANT INJECTION MODEL ON COOLED HIGH-PRESSURE VANES IN LARGE EDDY SIMULATION

M. Harnieh, M. Thomas, R. Bizzari, L. Gicquel and F. Duchaine

CERFACS CFD Team
harnieh@cerfacs.fr

Abstract

Combustion temperatures in modern gas turbine engines reach levels well above the thermal stress limit of materials used today applied in chamber and high-pressure turbines. Being the most critical component of the engine, the high-pressure turbine blades are therefore equipped with cooling system to ensure safe and longterm operation. To predict the flow in such configurations, Reynolds Average Navier Stokes (RANS) is usually used in the industrial context but is limited by its steady formalism. Potential improvement is foreseen with the Large Eddy Simulation (LES) which resolves the most energetic turbulent structures while modeling the small ones and has been found to be well suited to predict turbulent and fully unsteady flows. However, assessing the impact of a cooling system on the flow field of the high-pressure turbine using high fidelity simulations still remains prohibitively expensive. This work investigates the applicability for turbine cooled blades of a recently proposed effusion cooling model, designed for modeling cooling of the combustion chamber liners. This model was specifically designed to mimic the impact of cooling jets and do not require to solve the flow in the liners which leads to a dramatic reduction of the CPU cost.
To assess the applicability of the model on turbine blades, the cooled NGVs of the FACTOR configuration are chosen. A modeled LES using the hole model is carried out and compared to a hole-resolved LES on the same configuration. Results show that both simulations give very close results. The time averaged skin temperature of the model LES is slightly lower than the resolved one. Indeed, the cold film around the NGVs is colder and thinner with the model. Indeed, investigation of the RMS fields also shows that the turbulent mixing is less important if applied the model to blades.

1 Introduction

To comply with new environmental regulations and to reduce fuel consumption, the thermal efficiency of gas turbines has been improved by increasing the temperature at the exit of the combustion chamber. As a result, the thermal load on the Nozzle Guide Vanes (NGV) has increased dramatically. Indeed, the combustion temperatures in current burners surpass the thermal stress limits of the nozzle which makes the need for sophisticated cooling systems. The numerical prediction of the cooling efficiency on a cooled blade remains however a challenge today. Reynolds Average Navier-Stokes (RANS) simulations have been used in the past decades to predict the thermal load on blades but suffer from lack of accuracy in the prediction of the mixing between hot gases and injected coolant fluid in Li et al. (2015) [1]. This leads to the fact that meshing the inside and the outside of a blade is expensive. Film cooling models have so been implemented in RANS in Andrei *et al.* (2016) [2]. In parallel, Large Eddy Simulations (LES) resolving the most energetic turbulent structures, explained by Sagaut (2000) [3], are being increasingly used to predict turbulent flows in turbomachinery studied by Tucker (2011) [4]. However, resolving the entire NGV cooling system in LES needs a large number of cells to resolve the flow in the cooling system mesh compared to RANS. To alleviate associated cost, Bizzari *et al.* (2018) [5] have proposed a specific wall LES model to take into account the injection of coolant through liners in the combustion chamber. In the present work, this hole model is assessed in the specific context of the cooled NGV blades. In this approach, the cooling system is not meshed but projected on the surface of the blades allowing to save significant CPU resources. To assess the model, two simulations are carried out on the NGVs of the European project FACTOR (Full Aerothermal Combustor Turbine interactions Research) experimentally studied at the DLR (Germany) and UNIFI (Italia). The flow in the FACTOR configuration is highly swirled. The blades are cooled down by the cold flow coming from internal plenums and through 171 holes for each blade. First, a fully meshed configuration is considered, including the cooling system, i.e, the plenums and the holes. Then, a second computation using the hole model removing the internal feeding plenum is produced. In the following, the first computation will be referred as the resolved simulation and the second computation as the modeled simulation.

2 Numerical method

The computational domain retained represents an 18° sector (1/20 of the full annular domain) of the FACTOR high-pressure nozzle section containing 2 NGVs as shown on Fig. 1. The computational domain is limited by axial plane P40 located 17 mm upstream the blades and the outlet located at 6 blade chords downstream the blades. The mesh for the resolved LES is composed of 73 million of tetrahedra including 35 million of elements to mesh the cooling system. To ensure the resolution of the flow, an adaptive mesh refinement process has been applied to refine the mixing regions between hot flow and coolant jets using Daviler *et al.* (2017) [6] and the MMG3D libraries from Dapogny (2013) [7]. For the modeled simulation, the mesh on the blade surface is uniform and the holes as well as the plenums are not meshed. The resulting CPU cost is divided by 3 as presented in Table 1 in comparison to the resolved case. The finite element numerical scheme TTG4A from Colin and Rudgyard (2000) is used for both computations, i.e, 3^{rd} order in space and 4^{th} order in time. Subgrid scale turbulent contributions are accounted for by the WALE model proposed by Nicoud and Ducros (1999) [8]. The operating point and associated boundary conditions are detailed in Table 2. The walls are treated using an adiabatic logarithmic wall law for both LES. The inlet boundary conditions is extracted from a LES of an integrated computation combustion chamber - uncooled NGVs and time averaged. The corresponding 2D map including a hot spot of temperature and a swirled flow is shown in Fig. 2. All inflow and outflow boundary conditions are relaxed to the imposed value with the NSCBC formalism from Poinsot and Lele (1992) [9]. The coolant mass flow rates Q_{m1} and Q_{m2} are imposed at the inlet of the plenums with a temperature set at $T_{cold} = 300K$. At the outlet, the surface averaged static pressure is imposed and the radial equilibrium is obtained naturally.

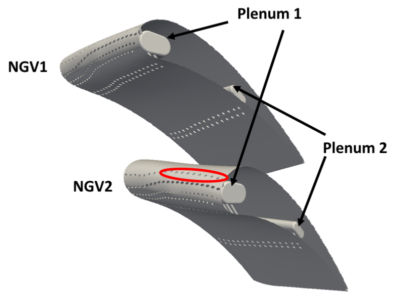

Figure 1: Description of the FACTOR NGV.

CASE	Cell number	CPU cost (HCPU)
Resolved LES	67.10^6	10 000
Modeled LES	37.10^6	3000

Table 1: Summary of the LES computations and CPU cost for one convective time.

Patch	Variable	Value
Inlet	Q_m	0.240 $kg.s^{-1}$
	T_{inlet}	455 K
Plenum 1	Q_{m1}	0.006 $kg.s^{-1}$
Plenum 2	Q_{m2}	0.003 $kg.s^{-1}$
	T_{cold}	300 K
Outlet	P_{outlet}	87000 Pa
Wall		Adiabatic wall law

Table 2: Boundary conditions used in the resolved LES. The inlet boundary condition is extracted and time averaged from the outlet of an integrated computation combustion chamber - NGV. The time and surface averaged values are indicated.

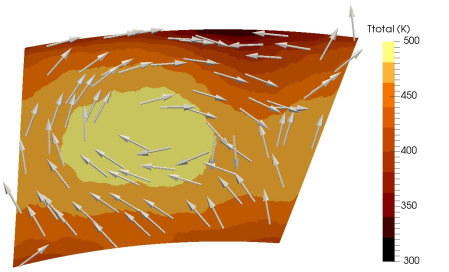

Figure 2: 2D temperature map including a hot spot and swirled flow imposed at the inlet boundary condition. Arrows evidence the swirled flow.

For the modeled simulation, the cold flow is directly imposed at the blade surface as shown on Fig. 3. Special refinement of the mesh at the cold flow injection is done to handle the locally strong gradients at the surface. To do so, 13 points are used to discretize the diameter of a hole. The mass flow rate and static temperature are imposed for each hole location. The velocity profile is imposed following a hyperbolic tangent function (see Bizzari *et al.* (2018) [5]) while the temperature profile is uniform. Such a modeling is however derived from multi-perforated liners that are clearly different from the one encountered here and deviations are expected. Indeed, the cooling in the context of turbine blades is different from the combustion

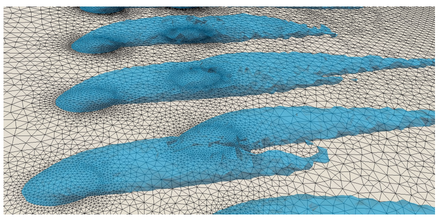

Figure 3: Isosurface of the cold temperature to evidence the cold flow in the modeled simulation.

chamber liners since the holes are larger with a different blowing ratio. The distribution of the cold mass flow on the blade surface originates from a RANS where the cooling system is resolved. Figure 4 assesses this cold mass flow distribution along the blade surface as obtained from the RANS and LES on the resolved cooling configuration. Clearly, both distribu-

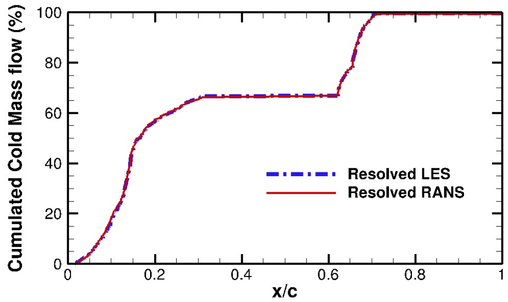

Figure 4: Cold mass flow distribution along the blade. Red solid line - represents the RANS simulations and blue dashed line -■- the resolved LES.

tions are in agreement. As a result, the modeled LES can be compared to the resolved LES as the cold flow distribution comes from the RANS simulation. For the comparison, the statistics are converged through 5 convective times based on the time averaged velocity along a streamline between the inlet and plane 41 defined 1.5 axial chords downstream the trailing edge.

3 Results

In this section, the operating point is first studied for both LES to ensure the comparison. Then, the flow organization is compared for the modeled and resolved LES. Then, total temperature profiles are investigated to quantify the effect of the model on the transport of the hot spot. Finally, the mixing between the hot and cold flow is detailed.

Table 3 displays the mass flow rate, total temperature T_t and pressure P_t differences between plane P40, corresponding to the inlet, and plane P41. Note that P_t and T_t are mass flow averaged. Both simulations in-

CASE	Resolved LES	Modeled LES
Hot mass flow rate	0.240	0.240
Cold mass flow rate	0.018	0.018
$P_{t40} - P_{t41}$ (Pa)	4673	4483
$T_{t40} - T_{t41}$ (K)	0.1	0.4

Table 3: Total variables drop between the planes P40 and P41. Mass flow rate are given in $kg.s^{-1}$.

ject the same mass flow rate for hot and cold gases. Since the coolant mass flow represents only 7.5 % of the total mass flow and the weak temperature differences, the total temperature drop remains very low for the two LES. The total pressure drop is however found to be more important for the resolved LES. That means that more losses are produced in the resolved LES.

The flow topology at the mid-height of the configuration is presented in Fig. 5. NGV1 (Fig. 1) is impacted

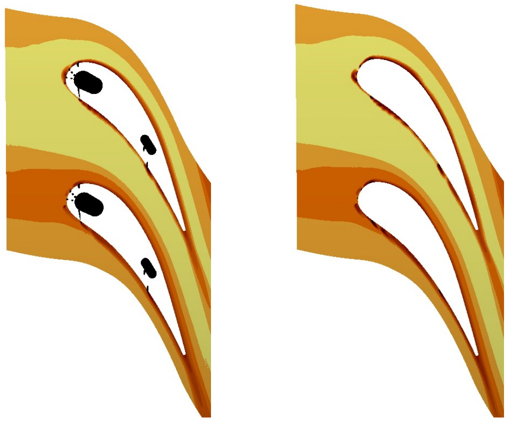

(a) Resolved LES. (b) Modeled LES.

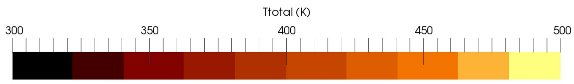

Figure 5: Time averaged total temperature field at the mid-height.

by the hot spot. Since the hot spot coincides with the center of the swirled flow, cold flow from NGV1 is expected to be more disturbed by the inlet than for NGV2. The total temperature maps are very similar except for the cooling flow topology. The jet penetration and thickness of the film seem to be different between the two LES. The flow is displayed at plane P41 in Fig. 6. For both cases, total temperature fields

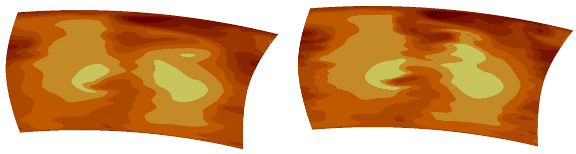

(a) Resolved LES. (b) Modeled LES.

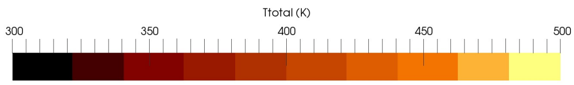

Figure 6: Time averaged total temperature field on plane P41.

are very similar. The flow is more uniform for the resolved LES. Indeed, in the modeled LES, the hot and cold gases appear more segregated indicating that the mixing between the main flow and the cold flow is less important in the modeled LES.

To assess the hot spot transport between planes P40 and P41, the total temperature is mass flow averaged in space for each radial position and the resulting radial profile is plotted on Fig. 7. At plane P40, no difference is noticed between both LES since the inflow

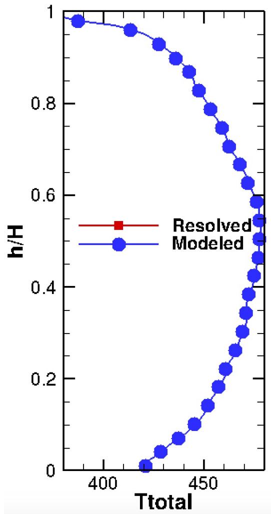

(a) P40.

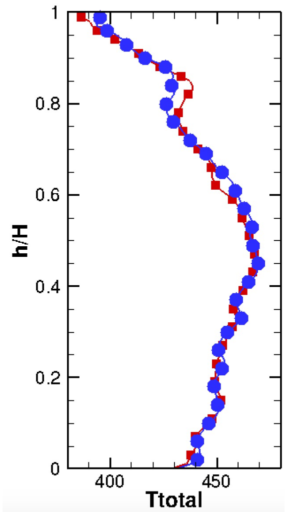

(b) P41.

Figure 7: Radial total temperature profile at the plane P40 and P41. Red solid line with squares represents the resolved LES and blue solid line with circle the modeled LES.

imposed is the same. At plane P41, the profiles appear very similar. Differences are noticed near the carter, between $0.6 < h/H < 0.8$.

The impact of the model on the skin temperature is displayed in Fig. 8. NGV1 skin temperature is strongly

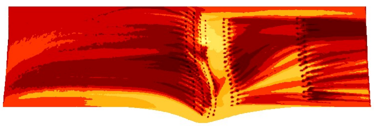

(a) Resolved NGV1.

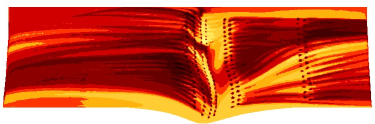

(b) Modeled NGV1.

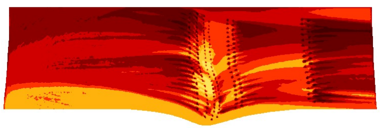

(c) Resolved NGV2.

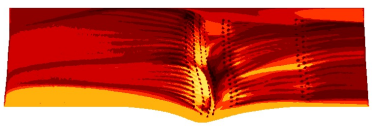

(d) Modeled NGV2.

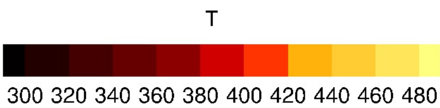

Figure 8: Time averaged temperature field on the skin blades of NGV1 and NGV2.

influenced by the swirled flow and the hot spot. The cold flow is indeed strongly deviated on NGV1. The skin temperature from the modeled LES is very comparable to the resolved LES. However, the traces of the jets on the blade surface are more coherent for the modeled LES indicating that the mixing with the hot flow is less efficient. The impact of the hot spot on the blade surface temperature seems influenced by the model. To quantify the impact on the skin temperature, the radial profiles of the skin temperature are plotted on Fig. 9 for both NGVs by averaging in space the total temperature for each radial position. The profiles

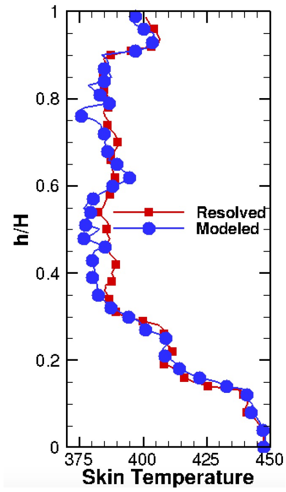

(a) NGV1.

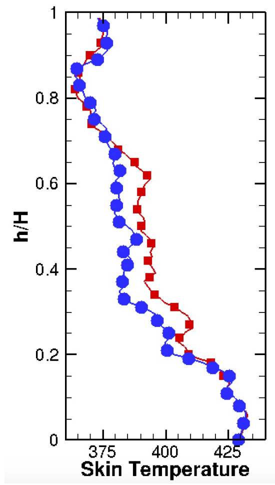

(b) NGV2.

Figure 9: Radial profile of the temperature skin for NGV1 and NGV2. Red solid line with squares represents the resolved LES and blue solid line with circle the modeled LES.

on NGV1 are very close with a maximum deviation of 10 K. The difference is more important on NGV2 over a larger radial extent. For both NGVs, the skin temperature is slighly colder with the model and the impact of the modeling is more important at mid-height than near the walls. The traces of the jets are more visible in the radial profile of the modeled LES indicating that less mixing occurs with the hot flow.

The film cooling topology is displayed near the leading edge of NGV1 in Fig. 10 for both LES. As clearly evidenced by this view, the cold flow does not separate from the wall for both LES. The jet penetration and the thickness of the cold film are slightly different. The thickness of the film δ, defined as the normal length from the wall up to $Y_{cooling} = 0.05$, is plotted on Fig. 11 at the mid-height for both NGVs and LES. For both NGVs, this thickness of the film is smaller for the modeled LES. The turbulent mixing is then less important for the modeled LES. The impact is more important on the pressure side. The no monotonous thickness evolution results from the swirled flow which distributes the cold flow in a complex heterogeneous way.

(a) Resolved LES.

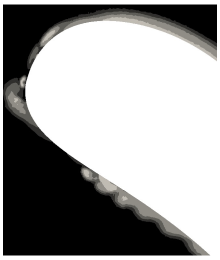

(b) Modeled LES.

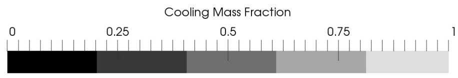

Figure 10: Cooling mass fraction near the leading edge of NGV1.

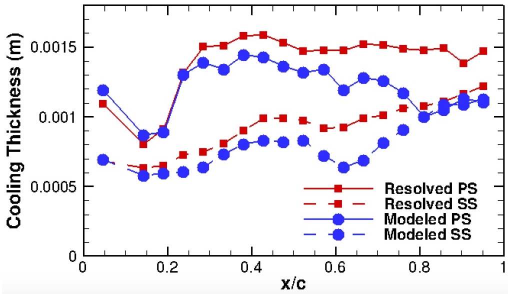

(a) NGV1.

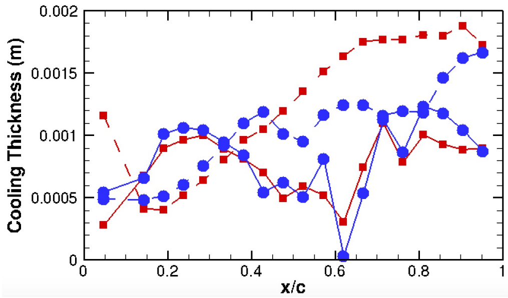

(b) NGV2.

Figure 11: Film thickness length along the blades. Red line with squares represents the resolved LES and blue line with circle the modeled LES. Solid lines represent the pressure side (PS) of the blades and dashed lines the suction side (SS) of the blade.

To illustrate, the mixing temperature, noted T_{mix}, in the film [10] can be evaluated from the temperature mass flow averaging in the film thickness,

$$T_{mix} = \frac{\int_0^\delta \rho U_i n_i T dn_w}{\int_0^\delta \rho U_i n_i dn_w} \tag{1}$$

where ρU_i is the mass flow per unit surface, n_i the normal aligned with the flow direction and n_W the normal coordinate from the wall. Resulting T_{mix} are plotted on Fig. 12 for both NGVs and both LES. The mixing temperature is colder for the modeled LES. It means that the hot gases interact less with the cold flow, keeping the film near the cold temperature. As a result, the

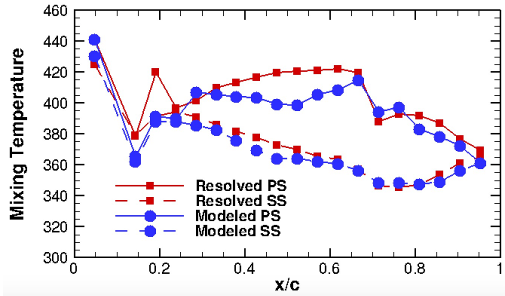

(a) NGV1.

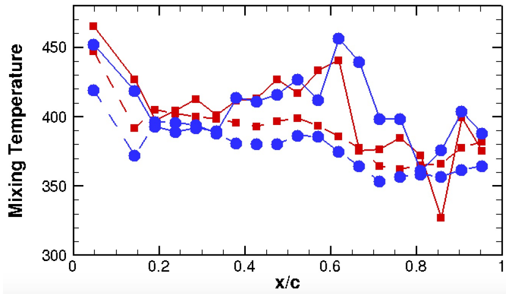

(b) NGV2.

Figure 12: Mixing temperature in the film along the blades. Red line with squares represents the resolved LES and blue line with circle the modeled LES. Solid lines represent the pressure side (SS) of the blades and dashed lines the suction side (SS) of the blade.

skin temperature is so colder with the model. To assess the turbulent mixing, maps of RMS fields of the temperature and the resolved turbulent kinetic energy maps are displayed on Fig. 13 and 14 at mid-height near the leading edge of NGV1. The T_{RMS} field

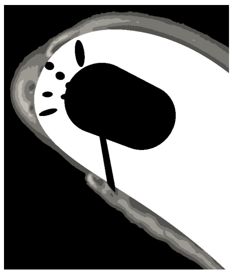

(a) Resolved LES.

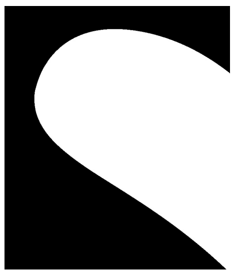

(b) Modeled LES.

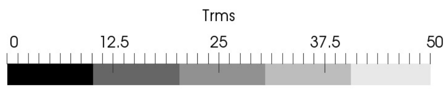

Figure 13: T_{RMS} map at mid height near the leading edge of NGV1.

shows that the turbulent temperature mixing is more important in the resolved LES than the modeled LES. This is also confirmed if looking at the turbulent kinetic energy maps (Fig. -14) which show that the turbulence is generated within the pipes and then transported to the freestream for the resolved LES, impact-

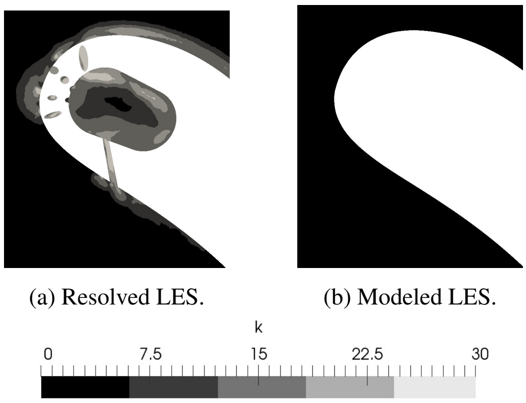

(a) Resolved LES. (b) Modeled LES.

Figure 14: Turbulent kinetic energy map at mid height near the leading edge of NGV1.

ing the film of cold flow and associated T_{RMS} production. Since the pipes are not meshed in the modeled LES, the turbulence created in the pipes is not present. As a result, turbulent mixing is significantly inferior in the modeled LES. The thickness of the film is then smaller and the film is colder.

4 Conclusion

In the present study, the applicability of the thickened-hole model on turbine blades has been assessed using a comparison between a fully hole-resolved simulation and a modeled one of the FACTOR NGVs. Results are very encouraging since both LES give very close results. This permits both an important CPU time saving and a design process enhancement compared to a resolved simulation where holes are meshed. Indeed, with the thickened-hole model, using a unique mesh of the blade, many hole layouts can be tested. However, as investigated in the present study, RMS fields show that the model should be improved since not enough RMS and mixing between the hot and cold gases are produced. As a result, the hot flow is less mixed with the cold flow. The skin temperature is hence colder when using the hole model. To improve the prediction of the mixing, it will be of interest to produce a fully unsteady injection model at the projected hole surface.

Acknowledgments

The authors wish to gratefully acknowledge FACTOR (Full Aerothermal Combustor-Turbine interactions Research) Consortium for the kind permission of publishing the results herein. FACTOR is a Collaborative Project co-funded by the European Commission within the Seventh Framework Programme (2010- 2017) under the Grant Agreement n° 265985. This work was granted access to the HPC resources of IDRIS under the allocation 2018 - A0032B10157 made by GENCI.

References

[1] Shuo Li, Jiemin Zhan, Yejun Gong, and Wenqing Hu. Numerical investigation of film cooling using rans and les. Procedia Engineering, 126:701–705, 2015.

[2] Luca Andrei, Luca Innocenti, Antonio Andreini, Bruno Facchini, and Lorenzo Winchler. Film cooling modeling for gas turbine nozzles and blades: Validation and application. Journal of Turbomachinery, 139:011004–011004–9, 2016.

[3] P. Sagaut. Large Eddy Simulation for incompressible flows. Scientific computation series. Springer-Verlag, 2000.

[4] P.G. Tucker. Computation of unsteady turbomachinery flows: Part 1 progress and challenges. Progress in Aerospace Sciences, 47(7):522 – 545, 2011.

[5] R. Bizzari, D. Lahbib, A. Dauptain, F. Duchaine, L.Y.M. Gicquel, and F. Nicoud. A thickened-hole model for large eddy simulations over multiperforated liners. Flow Turbulence and Combustion, Online First Articles:1–13, 2018.

[6] Guillaume Daviller et al. A mesh adaptation strategy to predict pressure losses in les of swirled flows. Flow Turbulence and Combustion, 99:93–118, 2017.

[7] Dapogny et al. Three-dimensional adaptive domain remeshing, implicit domain meshing, and applications to free and moving boundary problems. Technical report, 2013.

[8] F. Nicoud and F. Ducros. Subgrid-scale stress modelling based on the square of the velocity gradient tensor. Flow, turbulence and Combustion, 62(3):183–200, 1999.

[9] T. Poinsot and S. Lele. Boundary conditions for direct simulations of compressible viscous flows. Journal of computational physics, 101(1):104–129, 1992.

[10] R. Bizzari, D. Lahbib, A. Dauptain, F. Duchaine, S. Richard, and F. Nicoud. Low order modelling method for assessing the temperature of the multi-perforated plates. Submitted to Internation Journal of Heat and Mass Transfer, 2018.